Scientia Iranica C (2013) 20(6), 1912–1920

Sharif University of Technology
Scientia Iranica
Transactions C: Chemistry and Chemical Engineering
www.scientiairanica.com

Effects of viscoelastic polymer solutions on the oil extraction from dead ends

A. Kamyabi[a], A. Ramazani S.A.[b,*] and M.M. Kamyabi[b]

a. *Department of Chemical Engineering, Shahid Bahonar University of Kerman, Kerman, Iran.*
b. *Department of Chemical and Petroleum Engineering, Sharif University of Technology, Tehran, P.O. Box 11155-9313, Iran.*

Received 13 May 2012; received in revised form 13 November 2012; accepted 2 March 2013

KEYWORDS
Viscoelastic;
Oldroyd-B;
Leonov;
Polymer solution;
Numerical simulation;
Dead end.

Abstract. This research deals with the numerical simulation of two viscoelastic fluids flow in an open capillary of a reservoir. Oldroyd-B and Leonov models have been used to describe the rheological behavior of polymer solutions. The finite volume method on a structured and collocated grid has been used for discretization of the governing equations. The discrete elastic viscous stress splitting technique has also been used. The steady state, isothermal and incompressible fluids past through a two dimensional micropore have been considered. The numerical method has been validated through the comparison of numerical results by the analytical solutions of Oldroyd-B fluid flow through a planar channel. The effects of fluid characteristics and operating conditions on the oil sweeping from the dead ends are investigated. The contours of velocity, stream function and pressure are presented, and the swept depth is calculated. The presented results show that with increasing the Weissenberg number the swept depth of flooding fluid in the dead ends increases considerably. However, in the studied range, the Reynolds number does not have any significant effect on the sweep efficiency. The results also show that the swept depth in the case of viscoelastic fluids is more than the Newtonian and generalized Newtonian fluids.

1. Introduction

The petroleum industry recognized the problem of inefficient oil recovery by the conventional (primary and secondary) recovery methods in the early 1900s. After that, extensive researches have been conducted to improve the displacement and sweep efficiency of the oil recovery processes. Sweep efficiency is the ratio of oil extracted by flooding process to the remaining oil. Many different processes have been designed to improve the displacement efficiency by reducing the residual oil saturation in the reservoir. The residual oil means the oil which remains after flooding process. In the presented work both residual oil and sweep efficiency refer to their amounts only for dead-end, after complete flooding and becoming steady-state.

The water flooding is one of the oil recovery processes. However, this process has some drawbacks. One of them is the fingering problem in which water flows through the oil instead of pushing it. Muskat [1] found that this problem could be relatively solved by the mobility ratio correction.

Trapped oil in the dead ends within the porous media is the most part of the residual oil in a reservoir. The water flooding cannot displace or recover the trapped oil in the dead ends. However, in comparison, the polymer flooding is more effective in the oil sweeping from the open capillaries and dead ends because it has a favorable ratio in the mobility between the displacing and displaced fluids. Typically, there are four forms of residual oil in the reservoir: the oil droplet, the oil film, the oil in throats and the

*. *Corresponding author. Tel.: +98 21 66166405, Fax: +98 21 66022853.*
E-mail address: ramazani@sharif.edu (A. Ramazani S.A.)

oil trapped in the dead ends (see [2]). However, the residual oil available within the real pores are in many different and complicated forms.

Experimental results show that the polymer solutions enhance the displacement efficiency, but there are few theoretical studies on this subject, especially to determine the effects of polymer flooding on the oil recovery from the dead ends (see [3]).

Stiles [4] used the capacity distribution and permeability in the water flooding calculations. Dykstra and Parsons [5] studied the effects of mobility ratio and permeability variation on the oil recovery. Arnofsky [6] investigated the mobility ratio effects on the flood patterns during the water encroachment. Arnofsky and Ramey [7] studied injection and production histories in a five-spot water flooding process. Dyes et al. [8] showed the effects of mobility ratio on the oil production after the breakthrough. Afterward, Caudle and Witte [9] and Baranes [10] found that by increasing the water viscosity, the sweep efficiency of water flooding improves. However, it was Pye [11] and Sandiford [12] who, for the first time, found that the mobility of water (or brine) used in the water flooding process reduces efficiently by adding small amounts of a soluble polymer to the water flood.

Demin et al. [13] explored experimental data around oil sweeping from the dead ends for three kinds of fluids including viscous, high viscous and viscoelastic fluids. They show that viscoelastic fluids can remove the trapped oil in the dead ends more efficiently than Newtonian fluids. Jirui et al. [14] claimed that the interfacial tension between the polymer and the oil is not a major property for the polymer flooding. In the presented work, this simplification has been used to study one phase flow through micropore and extend the results to the two phase flow, as shown in [2]. Afsharpoor et al. [15] investigated the effect of viscoelastic fluids on the trapped droplet in pore throats. They found that normal forces could be dominate, and the total effective force would be enough to mobilize trapped oil. In the theoretical studies, geometry of the micropores are often simplified, e.g. an abrupt axisymmetric expansion, an abrupt axisymmetric contraction, rarely micropore with dead ends, etc. (see [3]). However, the expansion model is a typical model among them.

For the past several years, the numerical simulation of non-Newtonian flows has been carried out to understand their flow behavior in a variety of processes. Polymer fluids are of particular interest to the simulation community, because they have wide applications in the material processing, and their individual behavior is often complex and strikingly different from the Newtonian fluids. Unlike the Newtonian fluids, the polymeric liquids have some memory of the deformation they have experienced. The Newtonian fluids respond virtually instantaneously to the imposed deformation rate, whereas the viscoelastic polymeric fluids respond on a macroscopically large time scale, known as the relaxation time.

The finite volume method based on the pressure-correction strategy has been extensively and successfully employed for the Newtonian fluids flow and the heat transfer problems for more than three decades. In recent years, FVM has been improved gradually in order to solve non-linear non-linear flow problems involving the viscoelastic fluids. Benefiting from the Finite Volume Method (FVM) efficiency in terms of the memory and CPU time requirement compared to some other conventional numerical methods, such as the finite element methods, it is possible to carry out some complex three-dimensional (3-D) viscoelastic calculations on an ordinary workstation. The restriction to the regular geometries can be effectively removed by using unstructured mesh systems. Using FVM and Discrete Elastic Viscous Stress Splitting (DEVSS) benefits, oil sweeping from a dead end has been investigated in the presented work. The OpenFOAM code has been used and developed to implement the mentioned features.

2. Governing equations

The conservation of mass and momentum equations (neglecting the gravitational forces) can be written as follows [16]:

$$\nabla.\mathbf{V} = 0, \tag{1}$$

$$\rho D\mathbf{V}/Dt = -\nabla p + \nabla.\tau, \tag{2}$$

where $\mathbf{V}$ is the velocity vector, $D\mathbf{V}/Dt$ is the material or total derivative of the $\mathbf{V}$, ρ is the density of fluid, p is pressure and τ is deviatoric stress tensor. As Oldroyd-B model can predict normal stresses, and Leonov model can predict both normal stresses and shear thinning behavior; these models have been chosen to consider exactly viscoelastic effects of fluid on the sweep efficiency, and investigate the effects of normal stress and shear thinning behavior separately. Also, these models are used frequently in the polymeric simulations and have benefits to model a wide range of polymeric solutions.

Oldroyd-B constitutive equation is [17]:

$$\tau + \lambda_1 \overset{\nabla}{\tau} = 2\eta \left(\mathbf{V} + \lambda_2 \overset{\nabla}{\mathbf{V}} \right), \tag{3}$$

where λ_1 is the relaxation time, λ_2 is the retardation time, η is the zero shear rate viscosity, τ is the total-stress tensor, and $\overset{\nabla}{\tau}$ is the upper convected derivative of τ. The upper convected derivative of any symmetric tensor like A is defined by:

$$\overset{\nabla}{A} = \frac{\partial A}{\partial t} + \mathbf{V}.\nabla A - A.\nabla\mathbf{V} - \nabla\mathbf{V}^T.A, \tag{4}$$

and the rate of deformation tensor, $\mathbf{D}$, is given by:

$$\mathbf{D} = \frac{1}{2}\left(\nabla\mathbf{V} + \nabla\mathbf{V}^T\right). \tag{5}$$

When $\lambda_2 = 0$, Eq. (3) reduces to Upper Convected Maxwell (UCM) model, and if $\lambda_1 = \lambda_2 = 0$, it simplifies to the Newtonian fluid with the viscosity, η. If the stress tensor, τ, decomposed into a viscoelastic component, τ_p, and a purely viscous component, τ_s, then:

$$\tau = \tau_p + \tau_s, \tag{6}$$

where:

$$\tau_p + \lambda_1 \overset{\nabla}{\tau}_p = 2\eta_p\mathbf{D}, \tag{7}$$

and:

$$\tau_s = 2\eta_s\mathbf{D}. \tag{8}$$

Here, η_p is the viscosity of viscoelastic contribution, and η_s is the viscosity of Newtonian contribution. The relationship between parameters can be expressed as:

$$\eta = \eta_p + \eta_s, \tag{9}$$

and:

$$\lambda_2 = \frac{\eta_s}{\eta}\lambda_1. \tag{10}$$

Then, substituting Eqs. (7) and (8) into Eq. (6) and using Eqs. (9) and (10) results in Eq. (3). Afterward, the momentum equation can be written as:

$$\rho D\mathbf{V}/Dt = -\nabla p + \nabla.\tau_p + \eta_s\nabla^2\mathbf{V}. \tag{11}$$

After the similar procedure for the Leonov constitutive equation, its final form becomes as follows [18]:

$$\overset{\nabla}{\sigma} - \frac{1}{6\eta_p}\left(tr(\sigma) - \left(\frac{\eta_p}{\lambda}\right)^2 tr(\sigma^{-1})\right)\sigma = \frac{1}{2\eta_p}\left(\sigma.\sigma - \left(\frac{\eta_p}{\lambda}\right)^2 I\right), \tag{12}$$

$$\tau_p = \sigma - \frac{\eta_p}{\lambda}I, \tag{13}$$

where λ is the relaxation time, η_p is the zero shear rate polymer viscosity, σ is the transported stress, and τ_p is the polymeric-stress tensor. Similar to Oldroyd-B model, τ is obtained from Eq. (6).

Model equations could be non-dimensionalized, using the following nondimensional variables:

$$\mathbf{V}^* = \frac{\mathbf{V}}{\|\mathbf{V}_{in}\|}, \tag{14a}$$

$$p^* = \frac{Hp}{\eta\|\mathbf{V}_{in}\|}, \tag{14b}$$

$$\tau^* = \frac{H\tau}{\eta\|\mathbf{V}_{in}\|}, \tag{14c}$$

$$x^* = \frac{x}{H}, \tag{14d}$$

$$y^* = \frac{y}{H}, \tag{14e}$$

$$t^* = \frac{V_\infty t}{H}, \tag{14f}$$

$$\beta = \frac{\lambda_1}{\lambda_2}, \tag{14g}$$

where $\|\mathbf{V}_{in}\|$ is the magnitude of inlet velocity, H is the width of channel, β is the ratio of retardation to relaxation time. The value that β takes depends on the considered problem. Reynolds (Re) and Weissenberg (We) numbers are defined as:

$$\mathrm{Re} = \frac{\rho\|\mathbf{V}_{in}\|H}{\eta}, \tag{15}$$

$$\mathrm{We} = \frac{\lambda_1\|\mathbf{V}_{in}\|}{H}. \tag{16}$$

2.1. DEVSS methodology

DEVSS method has been chosen in the presented research to deal with the high Weissenberg number problem (see [19]). DEVSS method can be extended to different and complex constitutive equations. This method uses an additional variable. This new variable is defined as follows:

$$\mathbf{d} = \nabla\mathbf{V}. \tag{17}$$

Using this new variable, Eq. (11) can be written as follows:

$$\rho D\mathbf{V}/Dt - (\eta_s + \kappa)\nabla^2\mathbf{V} = -\nabla p + \nabla.\tau_p - \kappa\nabla.\mathbf{d}, \tag{18}$$

where κ is a positive number. The value of κ depends on the model parameters, but $\kappa = \eta_p$ is usually a good choice. It seems that adding the diffusion term to both sides of the equation has no effect. However, it affects the discretized form of equations. Adding Eq. (17) to the set of governing and constitutive equations will lead to a complete set of equations.

3. Computational approach

FVM method has been used to solve the flow equations. The equations are discretized using the second order schemes. The convective terms are discretized using QUICK scheme (see [20]). The diffusion terms are discretized using the central scheme, which is a second order scheme (see [21]). For simplicity at this point,

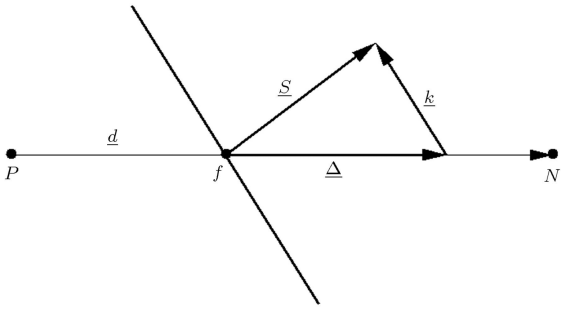

Figure 1. Non-orthogonality treatment.

a general transport equation has been considered as follows:

$$\underbrace{\frac{\partial \rho\phi}{\partial t}}_{\text{temporal derivative}} + \underbrace{\nabla.(\rho \mathbf{V}\phi)}_{\text{convection term}} - \underbrace{\nabla.(\rho\Gamma_\phi)\nabla\phi}_{\text{diffusion term}} = \underbrace{S_\phi(\phi)}_{\text{source term}} . \quad (19)$$

This equation is a representative form of the governing equations in the presented study. Γ_ϕ is the diffusion matrix. In the momentum equation, ϕ is $\mathbf{V}$. The details of the discretization are explained according to this equation and Figure 1.

3.1. Convection term discretization

One of the major issues in the discretizaion of convection term is to determine the value of ϕ on the shared face between two cells from the values in the cell centers. This study uses QUICK scheme of [20] with the van Leer limiter which is a second-order accurate scheme for the convection term. Second order schemes are associated with spurious oscillations, and first order ones have less accuracy. The basic concept of Limiters is mixing high order with low order schemes. Flux limiting is a procedure that creates a differencing scheme in order to include second order benefits without its disadvantages.

3.2. Diffusion term discretization

Using the assumption of linear variation of ϕ and the Gauss' theorem, the following is obtained:

$$\int_{V_P} \nabla.(\rho\Gamma_\phi\nabla\phi)dV = \sum_f \mathbf{S}.(\rho\Gamma_\phi\nabla\phi)_f = \sum_f (\rho\Gamma_\phi)\mathbf{S}.(\nabla\phi)_f. \quad (20)$$

In the cases that mesh is orthogonal, i.e. vectors $\mathbf{d}$ and $\mathbf{S}$ in Figure 1 are parallel, so:

$$\mathbf{S}.(\nabla\phi)_f = |\mathbf{S}|\frac{\phi_N - \phi_P}{|\mathbf{d}|}. \quad (21)$$

Using Eq. (21), the face gradient of ϕ can be calculated from the two values around the face. Unfortunately, mesh orthogonality is more an exception rather than a rule. In order to make use of the higher accuracy of Eq. (21), the product $\mathbf{S}.(\nabla\phi)_f$ is split into two parts:

$$\mathbf{S}.(\nabla\phi)_f = \Delta.(\nabla\phi)_f + \mathbf{k}.(\nabla\phi)_f. \quad (22)$$

The two vectors introduced in Eq. (22), Δ and $\mathbf{k}$, have got to satisfy the following condition:

$$\mathbf{S} = \Delta + \mathbf{k}. \quad (23)$$

The Δ vector is chosen to be parallel with the $\mathbf{d}$ vector. This allows the use of Eq. (21) on the orthogonal contribution, limiting the less accurate method only to the non-orthogonal part which cannot be treated in any other way.

The non-orthogonality error which violates the order of discretization comes into account only if it is necessary to guarantee the boundedness of the solution. In the presented study, because the mesh is orthogonal, the non-orthogonal component in Eq. (22) is discarded.

3.3. Source term discretization

Any terms of the equations that are not in the form of convection, diffusion or temporal terms are treated as sources. The source term, $S_\phi(\phi)$, can be a general function of the ϕ. Some general comments on the discretization of source term can be found in [22]. Before the discretization of the source term, it should be linearized as follows:

$$S_\phi(\phi) = S_u + S_p\phi, \quad (24)$$

where S_u and S_p could also depend on ϕ. After that, the volume integral is calculated as follows:

$$\int_{V_P} S_\phi(\phi)dV = S_u V_p + S_p V_p \phi_p, \quad (25)$$

where V_p is the volume of the control volume, and ϕ_p is the ϕ at the center of the control volume.

4. Flow in a planar channel

In this section, the flow of an Oldroyd-B fluid through a very long and planar (2-D) channel is simulated. Channel width and length are H and $20H$, respectively. The y direction is perpendicular to the channel length. The origin of axis is at the center of channel, between the walls. Analytical solution in the case of fully developed flow exists for this problem (see [16]). No-slip condition was imposed on the solid boundaries. At the outflow, the pressure was set to zero, and the homogeneous Neumann boundary conditions were imposed for the stresses. τ_{xx} and τ_{xy} at a cross section of the channel, where the velocity is fully developed, has been

compared with the analytical solution at different We numbers. The results show good agreement with the analytical solutions.

The equations were solved as a steady state and isothermal creeping flow (Re $\ll$ 1). The flow was simulated initially for We = 0.1 and $\beta = 1/11$. The We number was then incremented consecutively, and the previous solution of any state has been used as the initial guess for the new state.

To test the accuracy of the results, the normal and shear stresses at the steady state are compared with the analytical solutions. The analytical solutions for stresses are:

$$\tau_{xx} = 2\lambda\eta_p(\frac{\partial V_x}{\partial y})^2, \tag{26}$$

$$\tau_{xy} = \eta_p(\frac{\partial V_x}{\partial y}). \tag{27}$$

Figures 2 and 3 show the calculated normal and shear stresses along the y direction at a cross section near the end of channel at the fully developed region. The figures show that the numerical values are in agreement with the analytical solutions at different We numbers. The l_2 errors are presented in Table 1. The accuracy

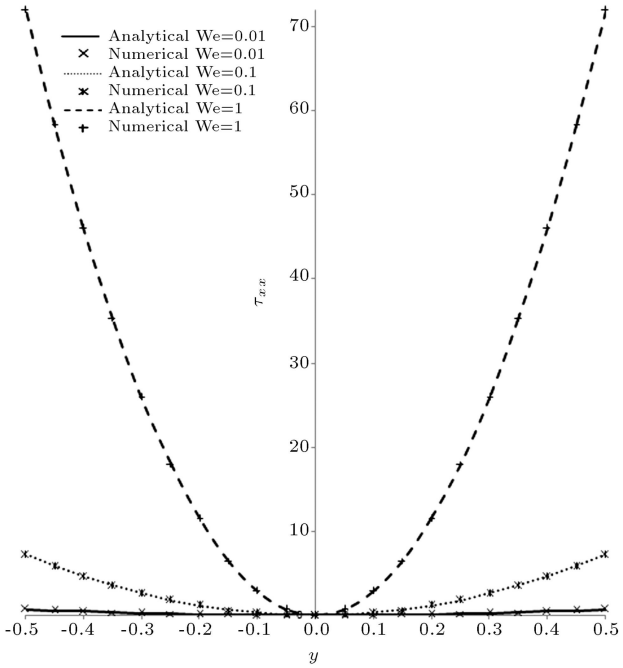

Figure 2. The analytical and numerical plots of τ_{xx}.

Table 1. The l_2 errors for τ_{xx} and τ_{xy}.

	We=0.01	**We=0.1**	**We=1**
τ_{xx}	1.3×10^{-4}	5.6×10^{-3}	3.4×10^{-2}
τ_{xy}	4.2×10^{-5}	8.9×10^{-4}	1.1×10^{-2}

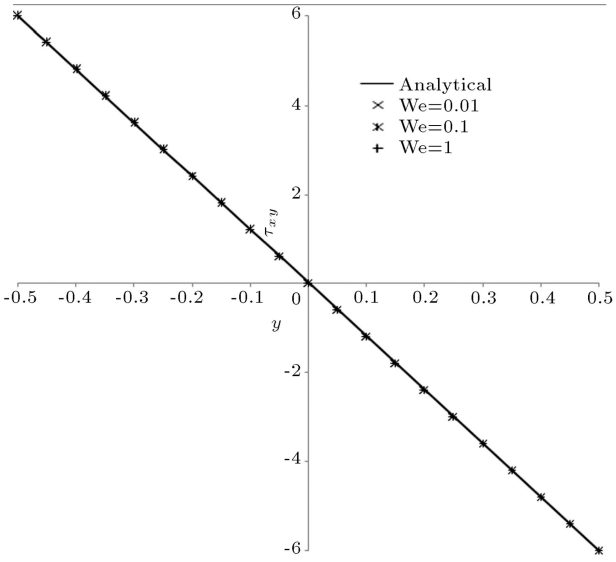

Figure 3. The analytical and numerical plots of τ_{xy}.

of results proves the robustness of algorithm in dealing with the viscoelastic fluid flows.

5. Flow in a channel with the dead end

Flow through a micro pore with the dead end is simulated in this section. Effects of the fluids and the operating conditions on the oil sweeping efficiency have been investigated. The micropores of an actual reservoir are very complicated. Residual oil exists in different forms in real reservoirs [2]. The most part of the residual oil is trapped in the dead ends of porous media. The micropores are often simplified in the numerical simulations. Figure 4 illustrates a simplified micropore with a dead end. A two-dimensional (2-D) and steady state flow of an isothermal and incompressible fluid with an inlet uniform velocity from left to right, according to Figure 5, has been considered.

5.1. Boundary conditions

To ensure that the solution is unique for a set of differential equations, the boundary conditions should be applied. In this case, the boundary conditions are as follows:

1. At the inlet boundary, the uniform flow conditions

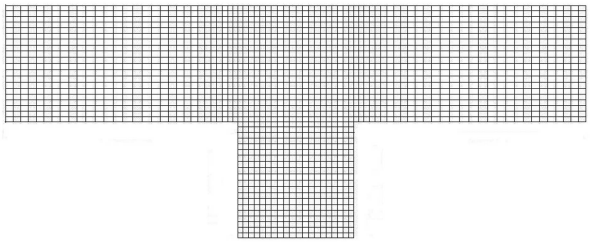

Figure 4. Schematics of the computational domain.

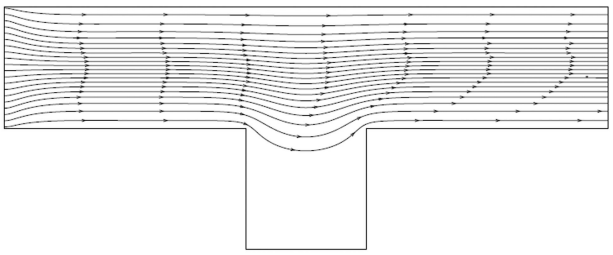

Figure 5. Sample of the stream lines plot for the Leonov model at the We = 0.1 and Re = 10^{-4}.

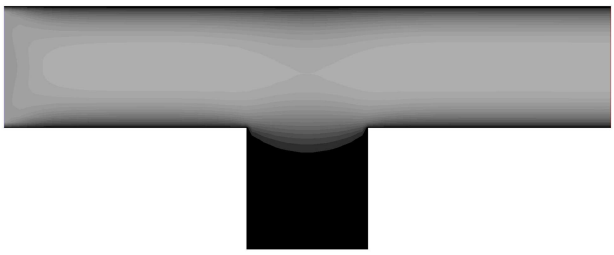

Figure 6. Velocity magnitude for the Leonov model at the We = 0.1 and Re = 10^{-4}.

are assumed:

$$V_x = 1, \qquad V_y = 0, \tag{28}$$

where, $\mathbf{V}$ is the dimensionless inlet velocity from left to right at the left vertical line in Figure 4.

2. At the walls of micropore, the no slip condition is assumed:

$$\mathbf{V} = \mathbf{0}. \tag{29}$$

3. At the exit boundary, the gage pressure is assumed to be equal to zero, and the homogeneous Neumann boundary condition is imposed for the extra-stress:

$$P = 0. \tag{30}$$

5.2. Numerical results

5.2.1. Mesh and numerical method

The mesh quality and independency are important issues in the validation of numerical simulations. So, in the presented work, simulations have been done with different mesh sizes, and finally the mesh size has been selected so fine that finer selection of the mesh size did not change, considerably, the numerical results. The finest grid in the presented study has about 1000 cells. Due to high velocity gradients in the inlet and near the walls, especially close to the corners of the dead end, the mesh has been produced adaptively with finest cells in the area of the maximum velocity gradient. This procedure could certainly handle the solution of equations at the high gradient fields, without considering too many cells which leads to efficient use of memory and CPU.

5.2.2. The stream lines and the velocity field

Considering a uniform velocity at the inlet results in the parallel and equal distance stream lines at the inlet, which can be verified in Figure 5. As shown in Figure 5, a few distances ahead of the inlet, the distance between the stream lines at the horizontal center line of the micro channel becomes smaller, and the distance between the stream lines near the walls becomes bigger. This is due to the boundary layer formation on the walls. As shown in Figure 6, small velocity magnitude at the end of the dead end is physically correct and makes sense. As the figure shows, near the dead end the velocity magnitude reduces at the horizontal center line of channel, because the cross section of channel at this point is bigger than other points. Therefore, the velocity magnitude reduces.

5.2.3. Effects of the Re on the sweep efficiency

For quantifying the sweep efficiency and making comparison between different conditions, sweep ratio has been used (see [23]). The sweep ratio definition is according to Eq. (31). As Figure 7 and Eq. (31) show, the sweep ratio is the ratio of swept depth to the depth of dead end. The effects of Re and We on the sweep ratio have been illustrated in Tables 2 and 3 for the Oldroyd-B and Leonov models, respectively. Tables 2 and 3 show that the sweep ratio is not sensitive to the Re number at the investigated conditions. Because, for the selected models, as the Re increases, the viscosity decreases. This is a good property for the flooding

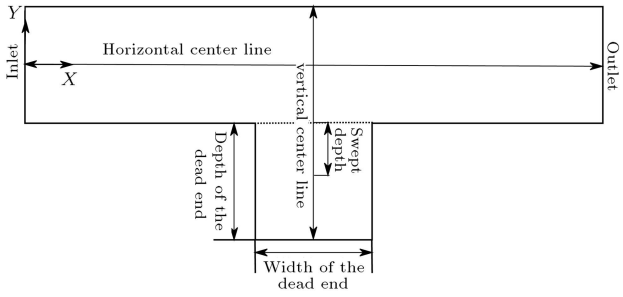

Figure 7. Sweep ratio definition.

Table 2. Sweep ratio for Oldroyd-B model.

	$\mathbf{Re = 10^{-3}}$	$\mathbf{Re = 10^{-4}}$	$\mathbf{Re = 10^{-5}}$	$\mathbf{Re = 10^{-6}}$
We=1	0.37	0.37	0.37	0.37
We=0.1	0.32	0.32	0.32	0.32
We=0.01	0.26	0.26	0.26	0.26

Table 3. Sweep ratio for Leonov model.

	$\mathbf{Re = 10^{-3}}$	$\mathbf{Re = 10^{-4}}$	$\mathbf{Re = 10^{-5}}$	$\mathbf{Re = 10^{-6}}$
We=1	0.36	0.36	0.36	0.36
We=0.1	0.30	0.30	0.30	0.30
We=0.01	0.25	0.25	0.25	0.25

fluid, because dimension of the pores in the reservoir are very different. Therefore, there is a wide range of Re in the pores of the reservoir. However, the polymer solutions have good efficiency in oil sweeping from the dead ends, independent of dimension of the pores.

$$\text{Sweep Ratio} = \frac{\text{Swept Depth}}{\text{Depth of the Dead End}}. \quad (31)$$

5.2.4. Effects of the We on the sweep efficiency
As Tables 2 and 3 show, We number has direct effects on the sweep ratio. This means that by increasing the We number, sweep ratio increases too. In other words, by increasing the elastic properties of polymer flood, the ability of polymer solution for oil sweeping from the dead ends increases.

5.2.5. Effects of the fluid
The effects of the Newtonian and generalized Newtonian fluids on the sweep efficiency have been presented in [23]. In order to compare viscoelastic fluids with generalized Newtonian and Newtonian fluids, Ref. [23] has been used. According to Ref. [23], sweep ratio is about 0.25 for the Newtonian fluids at all operating conditions. A comparison between the obtained results in Table 4 and the presented results in [23] shows that the sweep ratio in the case of viscoelastic fluids is more than that of generalized Newtonian and Newtonian fluids. Therefore, the use of viscoelastic solutions in the polymer flooding process is recommended. A comparison between Tables 2 and 3 shows that, the sweep efficiency in the case of Oldroyd-B model is slightly more then that of Leonov model, which could be due to higher normal stress differences for the Oldroyd-B model at the investigated conditions.

5.2.6. Contours of the first normal stress difference
Figure 8 shows the first normal stress difference for Oldroyd-B model at two different We numbers. As the figure shows, the first normal stress difference at the upper wall is at its maximum value, and it could be

Table 4. Sweep ratio for Leonov, Oldroyd-B and Carreau models at different We numbers.

	Carreau	**Leonov**	**Oldroyd-B**
We=1	0.20	0.36	0.37
We=0.1	0.25	0.30	0.32
We=0.01	0.25	0.25	0.26

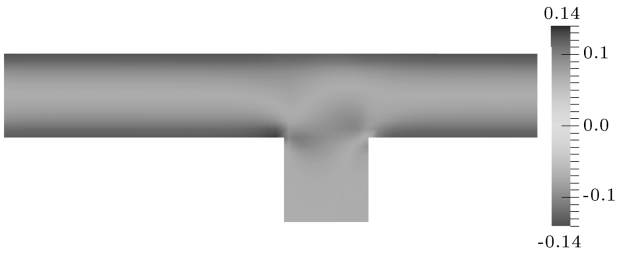

(a) We=0.01

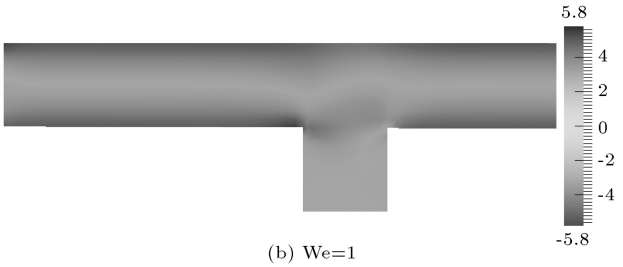

(b) We=1

Figure 8. Contours of the first normal stress for Oldroyd-B model at different We numbers.

the driving force for producing flow patterns, which can be seen in Figure 5. From the presented pattern in Figure 5, it can be concluded that the hole pressure (see [24]) is the driving force for the oil sweeping from the dead ends. As Figure 8 shows, the more the We number, the more the hole pressure will be.

It seems that the viscoelastic nature of the polymeric solution and their normal forces are the major reasons of better sweep efficiency of polymer flooding, in comparison to water flooding as one can find from presented data. Additionally as illustrated, the Re number has minor effects on the sweep efficiency, and it means that changing the viscosity could not enhance the sweep efficiency considerably. These results are in good agreement with [13].

5.2.7. Contours of the pressure
As Figure 9 shows, at the corners of inlet, there are high pressure changes. High curvature of the stream lines in the inlet confirms this phenomenon. At the end of channel, the pressure change is linear, which is almost true for the laminar flow in the long channels.

The figures do not show considerable vertical pressure changes. This could be due to ignoring the gravitational forces in the momentum equation. As Figure 9 shows, the pressure in the right vertical wall of the dead end is higher than that of the left one, and

Figure 9. Pressure contours for Leonov model at We = 0.1 and Re = 10^{-5}.

this is due to the fluid stagnation at the right vertical wall.

6. Conclusions

Presented results show that the viscoelastic fluids have the ability to extract the trapped fluid in the dead end much more than the Newtonian and generalized Newtonian fluids. Another important result is that, at the investigated range of Re number, Re has minor effects on the sweep efficiency. However, by increasing the We number, sweep efficiency increases considerably. These are very good properties for the polymer flooding process. There is many different length scales in the reservoir. Therefore, there is a wide range of Re number in the reservoir. However, in all investigated Re numbers the sweep efficiency for the viscoelastic fluids is more than that of the Newtonian and generalized Newtonian fluids. Therefore, the viscoelastic behavior of the fluid is more important than the operating conditions in the polymer flooding.

References

1. Muskat, M., *Physical Principles of Oil Production*, McGraw-Hill, New York (1949).
2. Zhang, L., Yue, X. and Guo, F. "Micro-mechanisms of residual oil mobilization by viscoelastic fkuids", *Pet. Sci.*, **5**, pp. 56-61 (2008)
3. Hongjun, Y., Demin, W. and Huiying, Z. "Study on coelastic polymer solution in micropore with dead end", *SPE*, **101950**, pp. 1-10 (2006).
4. Stiles, W.E. "Use of permeability distribution in water flood calculations", *Trans. AIME*, **186**, pp. 9-13 (1949).
5. Dykstra, H. and Parsons, R.L., *The Prediction of Oil Recovery by Water Flood*, API, New York, pp. 1-20 (1950).
6. Aronofsky, J.S. "Mobility ratio - Its influence on flood patterns during water encroachment", *Trans., AIME* 195, pp. 15-241 (1952).
7. Aronofsky, J.S. and Ramey, H.J. Jr. "Mobility ratio - Its influence on injection or production histories in five-spot water flood", *Trans., AIME*, **207**, pp. 205-210 (1956).
8. Dyes, A.B., Caudle, B.H. and Erickson, R.A. "Oil production after breakthrough as influenced by mobility ratio", *Trans. AIME*, **201**, pp. 81-86 (1954).
9. Caudle, B.H. and Witte, M.D. "Production potential changes duringsweep-out in five-spot system", *Trans. AIME*, **216**, pp. 448-449 (1959).
10. Baranes, A.L. "The use of a viscous slug to improve water flood efficiency in a reservoir partially invaded by bottom water", *Trans. AIME*, **225**, pp. 1147-1153 (1962).
11. Pye, D.J. "Improved secondary recovery by control of water mobility", *J. Pet. Tech. Trans. AIME*, **231**, pp. 911-916 (1964).
12. Sandiford, B. "Laboratory and field studies of water solutions to increase oil recoveries", *Trans. AIME*, **231**, pp. 917-922 (1964).
13. Demin, W., Jiecheng, C., Qingyan, Y., Wenchao, G., Qun, L. and Fuming, C. Viscous-elastic polymer can increase microscale displacement efficiency in cores", In *Society of Petroleum Engineers International Petroleum Conference*, Dallas, Texas (October 2000).
14. Jirui, H., Zhongchun, L. and Huifen, X. "Viscoelasticity of asp solutionis a more important factor of enhancing displacement efficiency than ultra-low interfacial tension in ASP flooding", *SPE*, **71061**, pp. 1-8 (2001).
15. Afsharpoor, A., Matthew, B.T., Bonnecaze, R. and Huh, C. "CFD modeling of the effect of polymer elasticity on residual oil saturation at the pore-scale", *Journal of Petroleum Science and Engineering*, **94-95**, pp. 79-88 (June 2012).
16. Edussuriya, S.S., Williams, A.J. and Bailey, C. "A cell-centred finite volume method for modelling viscoelastic flow", *Journal of Non-Newtonian Fluid Mechanics*, **117**, pp. 47-61 (2003).
17. Oldroyd, J.G. "On the formulation of rheological equations of state", *Number A200. Proc. Roy. Soc.*, London (1950).
18. Larson, R.G., *Constitutive Equations for Polymer Melts and Solutions*, MA, Butterworths, Boston (1988).
19. Guénette, R. and Fortin, M. "A new mixed finite element method for computing viscoelastic flow", *Journal of Non-Newtonian Fluid Mechanics*, **60**, pp. 27-52 (1995).
20. Leonard, B.P. "A stable and accurate convective modelling procedure based on quadratic upstream interpolation", *Comput. Methods Appl. Mech. Engrg.*, **19**, p. 5998 (1979).
21. Jasak, H. "Error analysis and estimation for the finite volume methodwith applications to fluid flows", PhD Thesis, University of London, UK (1996).
22. Patankar, S.V., *Numerical Heat Transfer and Fluid Flow*, Hemisphere Publishing Corporation (1981).

23. Kamyabi, A. and Ramazani, A.S.A. "Simulation of two generalized new-tonian fluid flow in micropore with dead end", *Computational Fluid Dynamics*, **25**(3), pp. 163-173 (March 2011).

24. Bird, R.B., Armstrong, R.C. and Hassager, O., *Dynamic of Polymeric Liquids*, John Wiley and Sons Inc., Canada (1987).

Biographies

Ata Kamyabi received his BS, MS and PhD degrees in Chemical Engineering in 2006 , 2008 and 2012 respectively from Sharif University of Technology, Tehran, Iran. He is currently Assistant Professor of Shahid Bahonar University of Kerman, Iran. His research interests include: CFD, rheology and multi phase fluids.

Ahmad Ramazani S.A. graduated from Laval University, Quebec, Canada, in 1999. He received his BS and MS degrees from Amirkabir University, Tehran, Iran. He is currently Professor of Department of Chemical and Petroleum Engineering at Sharif University of Technology, Tehran, Iran. His research interest is in interdisciplinary subjects mostly relating to experimental and theoretical investigation of polymer processing, polymer properties and flow of polymeric and non-newtonian fluids in different engineering fields including biomedical, nanotechnology and petroleum engineering media.

Mohammad Mahdi Kamyabi received his BS degree in Chemical Engineering from Sharif University of Technology, Tehran, Iran in 2011, where he is currently pursuing his M.Sc degree in Polymer Engineering. His research interests include: CFD, rheology and complex fluids.